Published in final edited form as:
Exp Physiol. 2012 February ; 97(2): 200–206. doi:10.1113/expphysiol.2011.058248.

Anoctamins and gastrointestinal smooth muscle excitability

Kenton M. Sanders, **Mei Hong Zhu**, **Fiona Britton**, **Sang Don Koh**, and **Sean M. Ward**
Department of Physiology and Cell Biology, University of Nevada School of Medicine, Reno, NV 89557 USA, (775) 784-6908 and FAX (775) 784-6903

Kenton M. Sanders: ksanders@medicine.nevada.edu

Abstract

Interstitial cells of Cajal (ICC) generate electrical pacemaker activity in gastrointestinal (GI) smooth muscles. We investigated whether *Tmem16a*, which encodes Anoctamin 1 (ANO1), a Ca^{2+}-activated Cl^- channel might be involved in pacemaker activity in ICC. *Tmem16a* transcripts and ANO1 were expressed robustly in GI muscles, specifically in ICC in murine, non-human primate (*Macaca fascicularis*) and human GI tracts. Splice variants of *Tmem16a* are expressed in GI muscles, as well as other paralogues of the *Tmem16* family. Ca^{2+}-activated Cl^- (CaCC) channel blocking drugs, niflumic acid and 4,4′-diisothiocyano-2,2′-stillbene-disulfonic acid (DIDS), blocked slow waves in intact muscles of mouse, primate, and human small intestine and stomach. Slow waves failed to develop in *Tmem16a* knock-out mice ($Tmem16a^{tm1Bdh/tm1Bdh}$). The pacemaker mechanism was investigated in isolated ICC from transgenic mice with constitutive expression of copGFP. Depolarization of ICC activated inward currents due to a Cl^- selective conductance. Removal of extracellular Ca^{2+}, replacement of Ca^{2+} with Ba^{2+}, or extracellular Ni^{2+} (30 μm) blocked the inward current. Single Ca^{2+}-activated Cl^- channels with a unitary conductance of 7.8 pS were resolved in excised patches from ICC. The inward current was blocked in a concentration-dependent manner by niflumic acid (IC_{50} = 4.8 μm). The role of ANO1 in cholinergic responses in ICC was also investigated. CCh activated Ca^{2+}-activated Cl^- currents in ICC, and responses to cholinergic nerve stimulation were blocked by niflumic acid in intact muscles. ANO1 is a prominent conductance in ICC and these channels appear to be involved in pacemaker activity and in responses to enteric excitatory neurotransmitters.

Keywords

Interstitial cells of Cajal; electrical rhythmicity; smooth muscle; gastrointestinal motility; enteric nervous system; Tmem16a

Introduction

Coordinated phasic contractions of smooth muscle cells are the basis for normal motor activities, such as peristalsis and segmentation, in the gastrointestinal (GI) tract. Phasic contractions are initiated and timed by electrical slow waves (Szurszewski, 1987) generated by interstitial cells of Cajal (ICC; Ward *et al*, 1994; Sanders, 1996). Slow waves are actively propagated within ICC networks and conducted to surrounding smooth muscle cells via gap junctions (Cousins *et al*, 2003). The amplitude of slow wave depolarization determines the opening of L-type Ca^{2+} in smooth muscle cells and thus the degree to which slow waves are coupled to phasic contractions. Slow wave amplitudes and, in some regions of the GI tract, slow wave frequency are regulated by excitatory and inhibitory enteric motor neurons. Inhibitory innervation is provided by neurons releasing nitric oxide, purines, and peptides, such as VIP or PACAP and excitatory neurons release acetylcholine and neurokinins, such as substance P or neurokinin A. Recent studies have shown that slow wave generation and regulation by excitatory neurons are mediated through Ca^{2+}-activated Cl^- channes, most

likely encoded by *Tmem16a*, in ICC of GI muscles (Zhu *et al*. 2009; Hwang *et al*. 2009, Gomez-Pinilla *et al*. 2009, Zhu *et al*, 2011). This brief symposium report reviews data supporting this conclusion.

Expression of Tmem16 splice variants and paralogues in the GI tract

Microarray analyses were performed to characterize the phenotype of ICC isolated from the murine small intestine (Chen *et al*. 2007). Genes expressed by ICC were compared to levels of expression in whole muscle tissues. A gene that emerged as one of the most highly expressed genes in ICC was transmembrane protein 16A (*Tmem16a*), which encodes anoctamin 1 (ANO1), a Ca^{2+}-activated Cl^- channel (Caputo *et al*. 2008; Schroeder *et al*. 2008; Yang *et al*. 2008). After the function of the proteins encoded by *Tmem16a* was discovered in 2008, antibodies to the ANO1 were tested to determine whether protein expression matched the expression of transcripts. These tests confirmed that ICC within the GI tracts of mice, humans and non-human primates (*Macaca fascicularis*) express ANO1 (Figure 1; Gomez-Panilla *et al*. 2009; Hwang et al, 2009). In the stomach and small intestine 2 populations of ANO1 positive cells were observed; one population was spindle shaped and found within the circular and/or longitudinal muscle layers (Hwang *et al*, 2009). Another population of cells, with multiple branching processes, was identified between the circular and longitudinal muscle layers. These cells formed an extensive network of cells in the myenteric region of the gastric corpus and antrum and throughout the small intestine (Figure 1). Double labeling with ANO1 and c-Kit antibodies showed that cells immunopositive for ANO1 were exclusively ICC (Hwang *et al*, 2009). In fact, ANO1 antibodies provide more specific labeling for ICC than c-Kit because c-Kit, but not ANO1, is also expressed by mast cells in the gut. Immunolabeling with antibodies to ANO1 was not resolved in muscles of W/W^V mice in regions of the gut lacking ICC. Figure 2 shows ANO1-like immunoreactivity in ICC of the murine small intestine.

We also evaluated the splice variants of *Tmem16a* expressed in the murine stomach and small intestine. Human *TMEM16A* is reported to express at least four alternatively spliced exons, named a, b, c and d (Caputo *et al*., 2008). We investigated whether similar splice variants occur in gastric and small intestinal *tunica muscularis* of mice. Primers that amplified across alternative exons were used for RT-PCR. Sequencing showed that all *Tmem16a* transcripts expressed in gastrointestinal muscles included the 12 bp “c” variant, and transcripts were present that included or excluded the 66bp “b” and 78bp “d” exon variants.

The *TMEM16* gene family consists of ten paralogues (*TMEM16a–h, j–k*; Rock & Harfe, 2008) in mammals. We investigated the expression of *Tmem16a* paralogues in murine gastric and jejunal muscles using RT-PCR and paralogue specific primers. Amplicons were detected of the expected molecular size for *Tmem16a, b, c, d, e, f, h, j* and *k* in all mouse GI muscles, but *Tmem16g* was not detected. It is possible therefore that cells other than ICC (e.g. enteric neurons which display Ca^{2+} activated Cl^- currents; Kang et al, 2003) might express other *Tmem16* and gene products may be responsible for the Cl− conductances in these cells. ICC may also express paralogues in addition to *Tmem16a*, however, as shown below, *Tmem16a* appears to be the dominant conductance driving slow waves in ICC.

Expression of Ca^{2+}-activated Cl^- current in ICC

We had not observed Ca^{2+}-activated Cl^- currents previously in studies of cultured ICC. Therefore, we utilized a new model of ICC in which mice were engineered to express a bright green fluorescent protein (copGFP) in ICC constitutively (Ro et al, 2010). Labeling with antibodies to c-Kit (a marker for ICC in GI muscles) showed that every cell with c-Kit-like immunofluorescence was also labeled with expression of copGFP (Fig. 2A&B). After

enzymatic dispersion, c-Kit$^+$ cells could be found in mixed cell population by green fluorescence (Fig. 2G–I).

ICC were studied under voltage-clamp conditions (Zhu et al, 2009) to determine whether freshly dispersed ICC displayed a conductance consistent with the expression of *Tmem16a* transcripts and channels. Cells were held at −80 mV and stepped to various potentials from −80 to +30 mV. Depolarization steps initiated large amplitude inward currents (−442±60 pA at maximum; −50 mV test potential). The currents reversed at about −20 mV in cells with physiological K^+ currents and at about 0mV when intracellular K^+ was replaced by Cs^+. The reversal potential shifted in a manner suggestive of a Cl^- current when the equilibrium potential for Cl^- was shifted from 0 to −40 mV (Figure 3). Large tail currents were apparent when membrane potential was stepped from the test potential back to the holding potential. Analysis of tail currents showed a reversal potential of −39±4 mV when E_{Cl} was adjusted to −40 mV. These experiments confirmed that the inward currents elicited in ICC were carried by Cl^- ions.

The Cl^- current in ICC displayed a very sharp increase in current over the range of −70 to −50 mV, and with steps more positive than −50 the current decreased and reversed in a linear manner as a function of the driving force on Cl^- ions. We also noted an odd property in the voltage-dependence of activation of the current. The current was activated to maximum over a narrow range of potentials near −70 mV. However, with small increment steps just positive to −70 mV we noted a delay in the activation of the current. Upon activation, the current reached maximal amplitude and displayed no voltage-dependence other than the initiation of the current. Both activation and inactivation profiles in response to voltage could not be fit with Boltzmann equations.

We concluded that an underlying conductance, possibly a small Ca^{2+} current provides an underlying voltage-dependent mechanism that activates Cl^- current in ICC. Reduction in extracellular Ca^{2+} or addition of Ni^{2+} (30 μM) blocked activation of the Cl^- current, and more recent experiments have confirmed the importance of a voltage-dependent Ca^{2+} current in the initiation of the Cl^- currents in ICC (Heifeng Zhang & K.M. Sanders, unpublished observations). Whole cell currents elicited in ICC were decreased from −761±75pA to −162±33pA by niflumic acid (10 μM). The IC_{50} for the block by niflumic acid was calculated to be 4.8 μM.

The Ca^{2+} dependence of the Cl^- conductance in ICC was demonstrated with excised patch recording of single channels. Channel openings of 7.8 pS Cl^- channels were observed in excised patches from ICC. This conductance is consistent with the conductance of ANO1 channels expressed in HEK cells (Yang *et al.* 2008). Ramp potential protocols from −80 to + 80 mV were applied, exposing the cytoplasmic surface of the patch to concentrations of Ca^{2+} from 10^{-6} to 10^{-8} M. Channel open probability was dependent upon Ca^{2+} concentration, and reversal potential was unaffected by Ca^{2+}. Current clamp experiments were also performed on isolated ICC. ICC discharged regular voltage transients in many cells (average 36±2 mV in amplitude at a frequency of 11.8±1.4 cycles per minute). These events are single cell electrical slow wave events. Thus, ICC display a spontaneous pacemaker mechanism. Niflumic acid (>10 μM) did not affect resting membrane potentials but inhibited spontaneous rhythmic voltage-transients. Thus, our data suggest that Ca^{2+}-activated Cl^- currents are fundamental to electrical rhythmicity in GI muscles.

Comparisons of the time-course and kinetics of the inward currents activated in ICC and the current-voltage relationship are considerably different than the currents attributed to ANO1 expressed in HEK293 cells (Hartzell *et al*. 2009). Activation of ANO1 currents in ICC, however, appears to depend upon the dynamics of cytoplasmic Ca^{2+} concentration ($[Ca^{2+}]_c$)

which have not yet been characterized during: i) voltage-dependent Ca^{2+} entry and ii) Ca^{2+} release events near the plasma membrane. Thus, without understanding the dynamics of changes in intracellular Ca^{2+} it is difficult to predict the exact characteristics and kinetics of a Ca^{2+}-dependent current. Careful measurements of Ca^{2+} ttransients have been made in many types of cells, and Fluo dyes are typically used as Ca^{2+} indicators such studies because of their properties. We have been unable to use Fluo 3 or Fluo 4 to monitor Ca^{2+} transients in ICC, because these cells are found in mixed cell dispersion by the expression of copGFP and the wavelengths of these indicators overlap. We have had no success with red Ca^{2+} indicators. Sub-cellular compartments within ICC may regulate the Ca^{2+} tied to ANO1 activation, and it may be difficult to monitor Ca^{2+} changes within these compartments accurately.

Role of Ca^{2+}-activated Cl^- currents in the electrical rhythmicity of intact muscles

The effects of Cl^- channel blocking drugs (niflumic acid and 4,4 diisothiocyanatostilbene 2,2′ disulfonic acid; DIDS) were tested on slow wave activity of gastric and small intestinal muscles from mouse and monkey (*Macaca fascicularis*) using intracellular microelectrode recording techniques (Hwang et al, 2009). These drugs inhibited slow waves in all GI muscles in a concentration-dependent manner. It is interesting to note that the potency of Cl^- channel blocking drugs differed in the stomach and small intestine. In general slow waves stomach muscles were far more sensitive to blockade by Cl^- channel blocking drugs than slow waves recorded from small intestinal muscles. The differences in sensitivity might be due to differences in the sensitivity of different splice variants of ANO1 channels that could be differentially expressed in the two regions of the gut.

Slow wave activity was also evaluated in mice homozygous with null *Tmem16a* alleles (*Tmem16a*$^{tm1Bdh/tm1Bdh}$, see Rock *et al*., 2008). These animals dies shortly after birth, so these tests were confined to the first week after birth. At birth slow waves were not resolved in *Tmem16a*$^{tm1Bdh/tm1Bdh}$ mice and electrical rhythmicity did not develop after 6 days in organ culture. Slow waves were normal in wildtype mice and in *Tmem16a*$^{+/tm1Bdh}$ mice. Two litters of mice were allow to develop for 23 days before sacrifice. Three *Tmem16a*$^{tm1Bdh/tm1Bdh}$ survived in these litters, but no slow waves resolved in tissues of these mice. A possible explanation for the lack of slow waves in these mice is that loss of Tmem16a could interfere with development of ICC. However, labeling of tissues from *Tmem16a*$^{tm1Bdh/tm1Bdh}$ showed normal numbers of ICC and no obvious differences in ICC or ICC network morphology. These data link expression of *Tmem16a* to generation of slow waves in ICC. Thus, it is likely that the Ca^{2+}-activated Cl^- currents measured in isolated ICC are responsible for slow waves in intact GI muscles (Zhu *et al*, 2009; Hwang *et al*, 2009).

Tmem16a expression and responses of ICC to neurotransmitters

Use of mutant animals with defective ICC networks (e.g. *W/W*^{V} and *Sl/Sl*^{d}) has made it possible to learn more about the physiological role of ICC. For example it was found that post-junctional responses to excitatory and inhibitory neurotransmitters was reduced in muscles of *W/W*^{V} and *Sl/Sl*^{d} lacking most intramuscular ICC in the gastric fundus (Ward *et al*, 2000;). However, it is possible that loss of ICC from birth might result in compensatory mechanisms that could cloud the full significance of these cells in neurotransmission (Sanders *et al*, 2010). We sought to determine whether the types of cells mediating cholinergic responses in GI muscle could be distinguished on the basis of the specific responses to neurotransmitter.

Previous studies have clearly shown that non-selective cation channels are activated in gut smooth muscle cells by muscarinic agonists (Benham *et al*. 1985; Inoue & Isenberg, 1990), and this conductance was recently shown to result from expression of canonical transient receptor potential (TRPC) channels, types 4 and 6 (i.e. TRPC4 and TRPC6; Tsvilovskyy *et al*. 2009). We have not observed Ca^{2+}-activated Cl^- currents in smooth muscle cells of small intestine or stomach. We investigated the effects of charbachol (CCh) on ICC to characterize the conductances activated by muscarnic stimulation.

Under current clamp conditions about ICC from the murine small intestine generated spontaneous transient depolarizations (STDs). CCh (100 nM – 1 μM) depolarized resting membrane potential and increased the frequency of STDs (Fig. 4A&B; Zhu *et al*, 2011). Niflumic acid and 5-nitro-2-(3-phenylpropylamino)-benzoic acid (NPPB; both 100 μM) hyperpolarized cells, blocked STDs and responses to CCh (Fig. 4C&D). Under voltage clamp spontaneous transient inward currents (STICs) were measured. STICs reversed at 0 mV when E_{Cl} was equal to 0 mV, and their reversal potential shifted to about −40 mV when E_{Cl} was adjusted to −40 mV. Current and voltage responses to CCh were also blocked by the muscarinic receptor antagonists atropine and 4-Diphenylacetoxy-*N*-(2-chloroethyl) piperidine hydrochloride (4-DAMP; M_3 antagonist). Taken together, these data suggest that STDs, and the STICs that underlie them, are due to spontaneous openings of Cl^- currents. Experiments on excised patches showed that the Cl^- conductance enhanced by CCh was Ca^{2+} dependent. Thus, it is likely that channels encoded by *Tmem16a* are responsible for the enhanced inward current activated in ICC by muscarinic agonists.

If different conductances are activated in smooth muscle cells and ICC by muscarinic stimulation, then it might be possible to determine which type of cell generates dominant responses to the ACh released from neurons. We compared electrical responses of intact muscles stimulated by either exogenous CCh or by stimulation of cholinergic neurons (Zhu *et al*, 2011). Stimulation of intrinsic motor neurons (0.3 ms duration pulses, 5 and 10 Hz; 10 sec trains) in the presence of, N^G-nitro-L-Arginine (L-NNA; 100 μM) and 2-Iodo-*N*6-methyl-(*N*)-methanocarba-2-deoxyadenosine-3′, 5′-bisphosphate (MRS2500; 1 μM) to inhibit enteric inhibitory neural inputs resulted in depolarization of intestinal smooth muscle cells and increased the maximal level of depolarization achieved during slow waves. These responses were blocked by atropine suggesting that they were due to release of ACh from motor neurons and binding of muscarinic receptors in post-junctional cells. Enteric excitatory responses were blocked by niflumic acid (100 μM). Exogenous CCh (in the presence of tetrodotoxin; 1 μM) caused depolarization of intestinal smooth muscles and increased the maximum level of depolarization attained during slow waves, responses that were quite similar in characteristics to responses to stimulation of enteric excitatory neurons. These responses were also blocked by atropine, but niflumic acid failed to block responses to CCh in intact muscles. These data suggest that ACh released from motor neurons primarily activates a Cl^- conductance, which our data demonstrates is expressed by ICC. In the presence of niflumic acid most of the response to ACh released from neurons was blocked. In contrast responses to whole muscles exposed to exogenous CCh are not strongly affect by niflumic acid because most of this response may be due to activation of non-selective cation conductances in smooth muscle cells. These data suggest that muscarinic regulation of GI muscles may depend upon expression of *Tmem16a* in ICC.

Further studies are needed to understand the Ca^{2+} dynamics in ICC to clarify the mechanism of spontaneous pacemaker activity in these cells and to understand the mechanisms of agonist responses in ICC. We are also seeking to construct a mouse with inducible CRE expressed specifically in ICC to test the role of specific receptors and ion channels in ICC and GI motility.

Acknowledgments

This project was supported by a research grants from NIDDK, DK41315 and DK40569. SMW was also supported by DK57236. Images were collected using a Zeiss LSM510 confocal microscope obtained with support from NIH1 S10 RR16871.

References

Beckett EA, Horiguchi K, Khoyi M, Sanders KM, Ward SM. Loss of enteric motor neurotransmission in the gastric fundus of *Sl/Sl*^{d} mice. J Physiol. 2002; 543:871–887. [PubMed: 12231645]

Benham CD, Bolton TB, Lang RJ. Acetylcholine activates an inward current in single mammalian smooth muscle cells. Nature. 1985; 316:345–347. [PubMed: 2410793]

Caputo A, Caci E, Ferrera L, Pedemonte N, Barsanti C, Sondo E, Pfeffer U, Ravazzolo R, Zegarra-Moran O, Galietta LJ. TMEM16A, a membrane protein associated with calcium-dependent chloride channel activity. Science. 2008; 322:590–594. [PubMed: 18772398]

Chen H, Ordog T, Chen J, Young DL, Bardsley MR, Redelman D, Ward SM, Sanders KM. Differential gene expression in functional classes of interstitial cells of Cajal in murine small intestine. Physiol Genomics. 2007; 31:492–509. [PubMed: 17895395]

Cousins HM, Edwards FR, Hickey H, Hill CE, Hirst GD. Electrical coupling between the myenteric interstitial cells of Cajal and adjacent muscle layers in the guinea-pig gastric antrum. J Physiol. 2003; 550:829–44. [PubMed: 12844505]

Gomez-Pinilla PJ, Gibbons SJ, Bardsley MR, Lorincz A, Pozo MJ, Pasricha PJ, Van de Rijn M, West RB, Sarr MG, Kendrick ML, Cima RR, Dozois EJ, Larson DW, Ordog T, Farrugia G. Ano1 is a selective marker of interstitial cells of Cajal in the human and mouse gastrointestinal tract. Am J Physiol Gastrointest Liver Physiol. 2009; 296:G1370–G1381. [PubMed: 19372102]

Hartzell HC, Yu K, Xiao Q, Chien LT, Qu Z. Anoctamin/TMEM16 family members are Ca2+-activated Cl− channels. J Physiol. 2009; 587:2127–2139. [PubMed: 19015192]

Hwang SJ, Blair PJ, Britton FC, O'Driscoll KE, Hennig G, Bayguinov YR, Rock JR, Harfe BD, Sanders KM, Ward SM. Expression of anoctamin 1/TMEM16A by interstitial cells of Cajal is fundamental for slow wave activity in gastrointestinal muscles. J Physiol. 2009; 587:4887–4904. [PubMed: 19687122]

Inoue R, Isenberg G. Acetylcholine activates nonselective cation channels in guinea pig ileum through a G protein. Am J Physiol. 1990; 258:C1173–C1178. [PubMed: 1694399]

Kang SH, Vanden Berghe P, Smith TK. Ca^{2+}-activated Cl^{-} current in cultured myenteric neurons from murine proximal colon. Am J Physiol Cell Physiol. 2003; 284:C839–C847. [PubMed: 12456397]

Ro S, Park C, Jin J, Zheng H, Blair PJ, Redelman D, Ward SM, Yan W, Sanders KM. A model to study the phenotypic changes of interstitial cells of Cajal in gastrointestinal diseases. Gastroenterology. 2010; 138:1068–1078. [PubMed: 19917283]

Rock JR, Harfe BD. Expression of TMEM16 paralogs during murine embryogenesis. Dev Dyn. 2008; 237:2566–2574. [PubMed: 18729231]

Rock JR, Futtner CR, Harfe BD. The transmembrane protein TMEM16A is required for normal development of the murine trachea. Dev Biol. 2008; 321:141–149. [PubMed: 18585372]

Sanders KM. A case for interstitial cells of Cajal as pacemakers and mediators of neurotransmission in the gastrointestinal tract. Gastroenterology. 1996; 111:492–515. [PubMed: 8690216]

Sanders KM, Hwang SJ, Ward SM. Neuroeffector apparatus in gastrointestinal smooth muscle organs. J Physiol. 2010; 588:4621–4639. [PubMed: 20921202]

Schroeder BC, Cheng T, Jan YN, Jan LY. Expression cloning of TMEM16A as a calcium-activated chloride channel subunit. Cell. 2008; 134:1019–1029. [PubMed: 18805094]

Szurszewski, JH. Electrical basis for gastrointestinal motility. In: Johnson, LR., editor. Physiology of the Gastrointestinal Tract. Raven Press; New York: 1987. p. 1435

Tsvilovskyy VV, Zholos AV, Aberle T, Philipp SE, Dietrich A, Zhu MX, Birnbaumer L, Freichel M, Flockerzi V. Deletion of TRPC4 and TRPC6 in mice impairs smooth muscle contraction and intestinal motility in vivo. Gastroenterology. 2009; 137:1415–1424. [PubMed: 19549525]

Ward SM, Beckett EAH, Wang X-Y, Baker F, Khoyi M, Sanders KM. Interstitial cells of Cajal mediate cholinergic neurotransmission from enteric motor neurons. J Neuroscience. 2000; 20:1393–1403.

Ward SM, Burns AJ, Torihashi S, Sanders KM. Mutation of the proto-oncogene c-*kit* blocks development of interstitial cells and electrical rhythmicity in murine intestine. J Physiol. 1994; 480:91–97. [PubMed: 7853230]

Yang YD, Cho H, Koo JY, Tak MH, Cho Y, Shim WS, Park SP, Lee J, Lee B, Kim BM, Raouf R, Shin YK, Oh U. TMEM16A confers receptor-activated calcium-dependent chloride conductance. Nature. 2008; 455:1210–1215. [PubMed: 18724360]

Zhu MH, Kim TW, Ro S, Yan W, Ward SM, Koh SD, Sanders KM. A Ca^{2+}-activated Cl^{-} conductance in interstitial cells of Cajal linked to slow wave currents and pacemaker activity. J Physiol. 2009; 587:4905–4918. [PubMed: 19703958]

Zhu MH, Sung IK, Zheng H, Sung TS, Britton FC, O'Driscoll K, Koh SD, Sanders KM. Muscarinic activation of Ca2+-activated Cl− current in interstitial cells of Cajal. J Physiol. 2011; 589:4565–4582. [PubMed: 21768263]

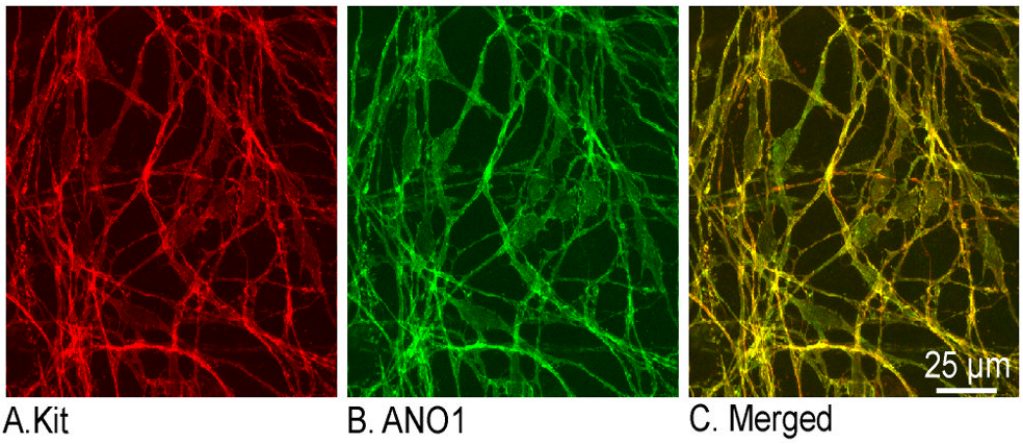

Figure 1. Expression of ANO1 in small intestinal muscles of *Macaca fascicularis*

Whole mount preparations were labeled with antibodies to c-Kit (red) and ANO1 (green). When the individual panels were merged there was a very high degree of co-localization of c-Kit- and ANO1-like immunoreactivity, suggesting ICC express this Ca^{2+}-activated Cl^{-} channels.

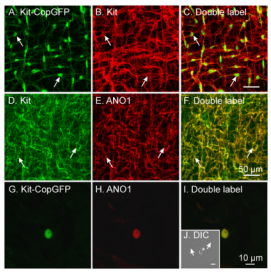

Figure 2. Expression of copGFP and ANO1 in ICC

Panel *A* shows copGFP^{+} cells in a whole mount preparation of the murine small intestine of Kit$^{+/copGFP}$ mice (green, arrows). copGFP fluorescence is primarily located in the perinuclear region of cells, but cellular are also labeled. Antibodies to c-Kit (red, Panel *B*) confirmed that copGFP^{+} cells are ICC (Panel *C*, merged images). Panel *D* shows c-Kit labeling in small intestine. Panel *E* shows ICC are labeled with antibody to ANO1. ICC are c-Kit- and ANO1-immunopositive (Panel *F*, merged images). When small intestinal muscles of Kit$^{+/copGFP}$ mice were dipersed with proteolytic enzymes, ICC could be detected by copGFP fluorescence (green cell; Panel *G*). These cells were also ANO1 immunopositive (red; Panel *H*). Panel I is a merged file of *G* & *H*. Panel *J*, an insert in Panel *I*, is a copGFP+ cell visualized with DIC. copGFP-negative cells were present in nearly every field. These cells were also ANO1-negative (arrows). Scale bar Panel *F* applies to *A*–*F*. Scale bar in Panel *I* applies to (applies to *G*–*I*). Scale bar in Panel *J* is 10 μm.

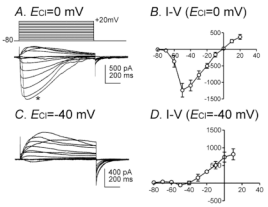

Figure 3. Whole cell currents in ICC dialyzed with Cs^+-rich solution pipette solution

ICC were dialyzed with Cs^+ solution to block contaminating currents carried by K^+ ions. Cells were depolarized from −80 to + 20 mV in 10 mV increments from a holding potential of −80 mV. When E_{Cl} was 0mV, inward currents were evoked at negative potentials and reversed at 0 mV (Panel *A*). Depolarization to −60 mV resulted in activation of inward current, but development of the current response (*) was delayed by 95 ms (see Zhu *et al*, 2009 for explanation of the delay in activation of the current). When E_{Cl} was adjusted to −40mV, outward currents were elicited by potentials positive to −40 mV (Panel *C*). Panels *B* and *D* show summary current-voltage (*I–V*) relationships; (n=6) and IV (n=4), respectively.

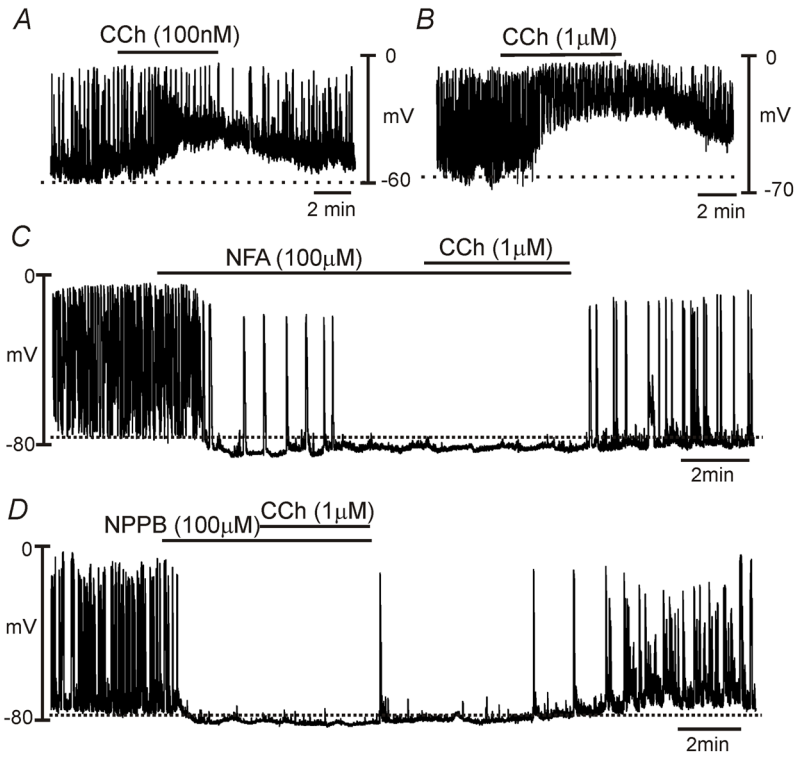

Figure 4. Effects of carbachol (CCh) on the resting membrane potential (RMP) and spontaneous transi*ent depolarizations (STDs) of ICC in current-clamp mode.*

A & B. CCh (100nM in **A**) and (1 μM in **B**) depolarized ICC and increased the frequency of STDs in ICC. ***C***. NFA (100 μM) induced hyperpolarization and decreased and eventually blocked STDs. CCh (1 μM) in the presence of NFA had no effect on RMP or STD generation. ***D***. NPPB (100 μM) induced hyperpolarization and blocked STDs. CCh (1 μM) in the presence of NPPB had no effect on RMP or STD generation.